J. Synchrotron Rad. (1998). **5**, 648–650

Optical design of the U7 undulator beamline at the Pohang Light Source

Hyun-Joon Shin,* Y. Chung and Bongsoo Kim

Beamline Research Division, Pohang Accelerator Laboratory, POSTECH, Pohang 790-784, Korea.
E-mail: shj001@vision.postech.ac.kr

(*Received 4 August 1997; accepted 10 November 1997*)

The first insertion-device beamline at the Pohang Light Source is designed for high-resolution spectroscopy and spectromicroscopy. The beamline will contain a variable-included-angle plane-grating monochromator (VIA-PGM) using a grating substrate which has seven different grooves with different depths. The advantages of this scheme will be the fixed exit-slit position and the mechanical stability of the grating scan mechanism while changing the photon energy range. The beamline is designed to cover the photon energy range 20–2000 eV. The estimated spectral resolution, $E/\Delta E$, is above 8000 in the photon energy range below 500 eV, and above 4000 for the remaining photon energy range. The estimated flux at the end-station is of the order of 10^{12} photons s^{-1} (0.1% bandwidth)$^{-1}$.

Keywords: beamline design; undulator beamlines; plane-grating monochromators.

1. Introduction

There is an increasing demand for high-brilliance soft X-rays for high-resolution spectroscopy and spectromicroscopy (Terminello *et al.*, 1996), and the first beamline with a general-purpose 50 μm spot diameter has been realized at the Advanced Light Source (Warwick *et al.*, 1995). Brilliant soft X-rays reduce data-acquisition time and enable scientists to obtain accurate information both on the materials themselves and on the transient mechanisms of surface reactions. The brilliant soft X-rays can be further focused down to a submicrometre scale (about 0.1 μm), incorporated with state-of-the-art X-ray optics such as Fresnel zone plates and used for the study of microstructures, alloys, chemical fibres *etc.* In order to meet these demands at the Pohang Light Source (PLS), the first insertion device, U7, has been fabricated and installed and the design for the undulator beamline has been completed. In this paper, we present the optical parameters and design of the U7 undulator beamline.

2. Optical design

The U7 undulator beamline is designed to be operational with an electron beam energy of 2.5 GeV and a current of 200 mA. The storage ring and undulator parameters are listed in Table 1. The expected spectral range of the useful undulator radiation is 40–700 eV in the first harmonic and 120–2100 eV in the third harmonic, with flux in the range 10^{14}–10^{15} photons s^{-1} (0.1% bandwidth)$^{-1}$. The r.m.s. size and divergence of the central cone X-rays were calculated by convoluting the electron beam size and divergence and the diffraction-limited source size and divergence (Kim, 1989).

Table 1
Storage ring parameters at the straight section.

Electron energy (e)	2.5 GeV
Period length (λ_u)	7 cm
Number of periods (N)	61
Horizontal emittance (ε_x)	18.9 nm rad
Vertical emittance (ε_y)	0.189 nm rad
β_x	10 m
β_y	4 m
Beam current (I)	0.2 A

The schematic layout of the U7 beamline is shown in Fig. 1. In the vertical direction (elevation view) the central cone X-rays are focused on an entrance slit (S1) by a toroidal mirror (M1). The beam is then deflected by a premirror (Mp) to provide the desired included angle or incidence angle at a grating (G). The diffracted beam from the grating is then focused by a focusing mirror (Mf) onto an exit slit (S2). The beam from the slit is refocused by a vertical refocusing mirror (Mv) onto two different branches: ES1 for high-resolution spectroscopy and ES2 for spectromicroscopy. In the horizontal direction (plan view) the beam is deflected by the toroidal mirror and then refocused by the switch-yard horizontal mirrors (Mh1 and Mh2) onto the two branches. The clear aperture of each optical component was chosen to be greater than two times the FWHM (full width at half-maximum) of the footprint of the central cone. The parameters of the mirrors are listed in Table 2.

In order to cover the photon energy range 20–2000 eV, a plane-grating substrate with seven different groove depths will be used. Each groove will have the same 700 lines mm^{-1} groove density and will be parallel to the beam path. This kind of grating can be fabricated by controlling the exposure time using a mask just above the substrate in the holographic-ruling method (ZEISS). The depth of each groove and the spectral range to be covered are given in Table 3. The depth of each groove was determined to give optimized diffraction efficiency for each spectral range (Martynov, 1996; Young, 1996). The 'width' of each groove is the ruled length in the direction perpendicular to the beam direction, and is larger than twice the expected FWHM size of the X-rays. The overall width of the grating is 55 mm. The main advantage of using such a wide grating will be realized when the photon energy range is changed; the grating need only be moved a few cm along

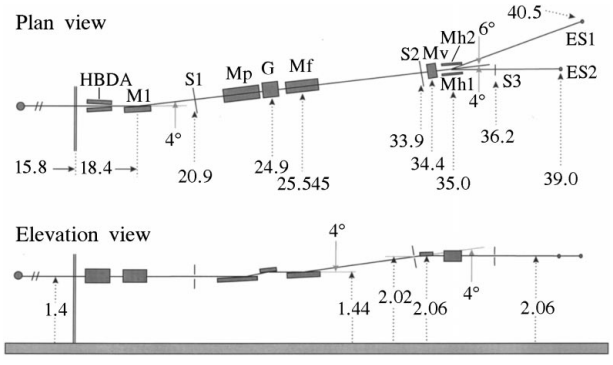

Figure 1
Schematic layout of the U7 beamline at the PLS, showing the main optical components. The numbers in the plan view are distances in metres from the undulator centre along the beam path, and the numbers in the elevation view are the heights of components from the floor. HBDA: horizontal beam-defining aperture.

Table 2
Optics parameters.

	M1	Mp	G	Mf	Mv	Mh1	Mh2
Shape	Toroid	Plane	Plane	Cylinder	Cylinder	Cylinder	Cylinder
Coating material	Au	Au	Au	Au	Au	Au	Au
Substrate	Glidcop	Si	Si	Glidcop	Glidcop	Glidcop	Glidcop
Cooling	Yes	Yes	Yes	Yes	No	No	No
Incidence angle (°)	2	Variable	Variable	2	2	3	2
Tangential radius of curvature (m)	1054.46	Infinite	Infinite	341.2	21–28	191–4000	46–287
Sagittal radius of curvature (m)	0.1536	–	–	–	–	–	–
Tangential slope error (μrad)	15	0.5	0.5	0.5	3	5.5	14
Sagittal slope error (μrad)	6	–	–	–	–	–	–
Surface roughness (nm)	0.6	0.5	0.5	0.5	0.6	0.5	0.6
Clear aperture (mm × mm)	320 × 50	750 × 50	150 × 50	700 × 50	100 × 40	230 × 40	230 × 40

Table 3
Groove depth and width of the plane grating.

Groove depth	Width	Photon energy
55 nm	10 mm	20–25 eV
40 nm	9 mm	25–45 eV
35 nm	8 mm	45–60 eV
27 nm	8 mm	60–100 eV
17 nm	7 mm	100–350 eV
11 nm	7 mm	350–900 eV
7.5 nm	6 mm	900–2000 eV

the direction perpendicular to the beam path. This leads to increased mechanical stability and reproducibility.

In order to have a fixed exit-slit position while scanning the photon energy, a VIA-PGM (variable-included-angle plane-grating monochromator) is adopted as a monochromator (Padmore, 1989; Padmore *et al.*, 1994; Young *et al.*, 1995). The prevailing equation of the monochromator is

$$\cos^2\beta/\cos^2\alpha = -r'/r = K_g^2. \quad (1)$$

In the equation, α and β are incidence and diffracted angles at the grating, r and r' are the distances between the entrance slit and the grating and between the grating and the virtual image, respectively. The constant K_g is set to 2.24. Using (1) and the grating equation

$$\sin\alpha + \sin\beta = Nk\lambda, \quad (2)$$

the incidence and diffraction angles at the grating and other parameters were determined. Fig. 2 shows the calculated values. In Fig. 2, 'premirror angle' is the angle of the premirror surface relative to the horizon and 'grating angle' is that of the grating surface relative to the horizon. 'Mp distance' is the distance along the horizontal direction from the centre of the grating surface to the beam position at the premirror. In the calculation, the height between the centre of the grating surface and the beam position at the premirror was set to 4 cm. The incidence angle at the grating, the grazing angle, is also shown in Fig. 2. The diffracted X-rays from the grating are then parallel to the horizon and incident on the focusing mirror. The incidence angle at the focusing mirror is 2°, and the beam is then reflected upward by 4° relative to the horizon and focused onto the exit slit.

The spectral resolution was calculated by considering the diffraction limit due to the illuminated width at the grating, the slope errors at the grating, the premirror and the focusing mirror, the comas of the grating and the focusing mirror, and the sizes of the entrance and exit slits. These contributions were convoluted, assuming Gaussian distributions, to give the total spectral resolution. The total spectral resolution is shown in Fig. 3, where the slope error of the grating is 1 μrad. In the calculation, the footprint of the X-rays at each optic was set to its FWHM value. The decrease in spectral resolution at higher photon energies is mainly due to the slope error of the optics and the slit sizes, and the decrease at lower photon energies is due to the coma of the focusing mirror. In practical situations the critical factor will be the slope errors at the optics while illuminated by the X-rays. The power of the undulator radiation will be high (maximum 285 W) and the thermal load on the premirror and the grating will not be negligible. In order to reduce thermal distortion, the premirror and the grating will have integrated internal cooling channels (Boeing North American, Inc.).

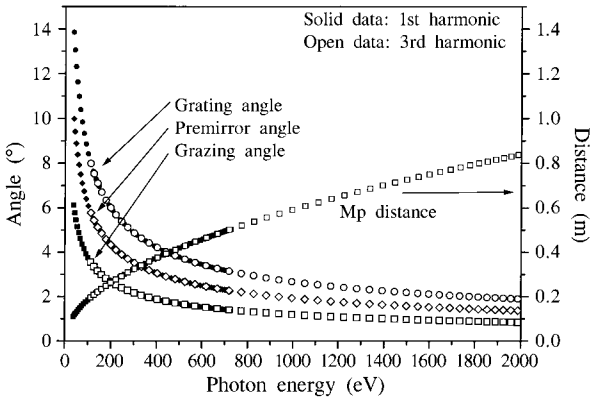

Figure 2
Premirror angle, grating angle, grazing angle at the grating and the distance along the horizontal direction from the centre of the grating surface to the beam position at the premirror.

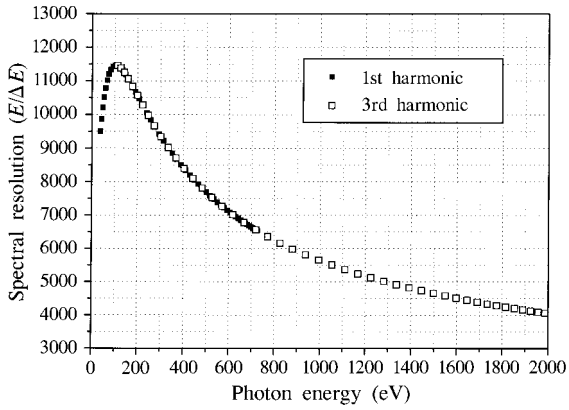

Figure 3
Total spectral resolution of the monochromator as a function of photon energy. The slope error of the X-ray optics is 1 μm.

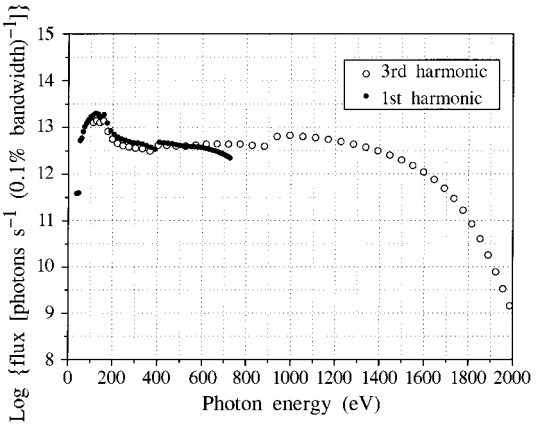

Figure 4
Flux at end-station ES2 as a function of photon energy.

The flux at end-station ES2 was calculated by considering the reflectivity at each mirror (Henke *et al.*, 1993), the throughput through the entrance slit due to the spherical aberration of the toroidal mirror, and the throughput of the monochromator and the reflectivity of the refocusing mirrors. The throughput of the monochromator was obtained by taking the reflectivity of the premirror and the focusing mirror, the diffraction efficiency of the grating and the throughput through the exit slit due to the spherical aberration from the focusing mirror. In calculating the diffraction efficiency, the grating was assumed to have a laminar-type groove-profile and a shadowing effect was applied (Bennett, 1971). The result is shown in Fig. 4 as a function of photon energy at an electron beam current of 0.2 A. For most of the photon energy range the expected flux at the sample is of the order of 10^{12} photons s^{-1} (0.1% bandwidth)$^{-1}$.

The size of the X-rays at the sample depends on the photon energy, and decreases as the photon energy increases. The expected size, at a photon energy of 44.6 eV, is 190 × 310 μm (FWHM) at the end-station ES1 and 55 × 140 μm (FWHM) at the pinhole (S3) of the end-station ES2.

3. Conclusions

The U7 beamline at PLS has been designed for high-resolution spectroscopy and spectromicroscopy. A VIA-PGM (variable-included-angle plane-grating monochromator) scheme has been adopted in order to achieve better performance in practical use. The main advantage of the VIA-PGM is the fixed exit-slit position while scanning the photon energy. The drawback of the addition of X-ray optics will be partly compensated by the higher diffraction efficiency. The use of one 55 mm-wide grating substrate with seven different groove depths will provide mechanical stability and reproducibility when the photon energy range is changed.

The performance of the beamline is estimated based on the undulator and X-ray optic parameters. The expected spectral resolution of the monochromator is about 8000 for the spectral range below 500 eV, and above 4000 for the remaining photon energy range. The photon flux at the end-stations is estimated to be of the order of 10^{12} photons s^{-1} (0.1% bandwidth)$^{-1}$ with a spot size of 190 × 310 μm (FWHM) at ES1, and of 55 × 140 μm (FWHM) at the pinhole (S3), at a photon energy of 44.6 eV.

References

Bennett, J. M. (1971). PhD Thesis, University of London, UK.
Henke, B. L., Gullikson, E. M. & Davis, J. C. (1993). *At. Data Nucl. Data Tables*, **54**, 181–342.
Kim, K.-J. (1989). *AIP Conf. Proc.* **184**, 565–632.
Martynov, V. (1996). Personal communication.
Padmore, H. A. (1989). *Rev. Sci. Instrum.* **60**, 1608–1615.
Padmore, H. A., Martynov, V. & Holis, K. (1994). *Nucl. Instrum. Methods Phys. Res. A*, **347**, 206–215.
Terminello, L. J., Mini, S. M., Ade, H, & Perry, D. (1996). Editors. *Applications of Synchrotron Radiation Techniques to Material Science III, Materials Research Society Symposium Proceedings*, Vol. 437. Pennsylavia: Materials Research Society.
Warwick, T., Heimann, P., Mossessian, D., McKinney, W. & Padmore, H. (1995). *Rev. Sci. Instrum.* **66**, 2037–2040.
Young, A. (1996). Personal communication.
Young, A., Hoyer, E., Marks, S., Martynov, V., Padmore, H. A., Plate, D. & Schlueter, R. (1995). LBNL Note 37765. LBNL, Berkeley, CA, USA.